Catalysis Today 154 (2010) 53–60

Contents lists available at ScienceDirect

Catalysis Today

journal homepage: www.elsevier.com/locate/cattod

Adsorption/desorption studies of CO on a rhodium(1 0 0) surface under UHV conditions: A comparative study using XPS, RAIRS, and SSIMS

Maarten M.M. Jansen *, Freek J.E. Scheijen, Jonathan Ashley, Ben E. Nieuwenhuys, J.W. Niemantsverdriet (Hans)

Schuit Institute of Catalysis, Eindhoven University of Technology, P.O. Box 513, 5600 MB, Eindhoven, The Netherlands

ARTICLE INFO

Article history:
Available online 24 December 2009

Keywords:
Carbon monoxide
Rh(1 0 0)
Surface science
Isosteric heat of adsorption
Equilibrium

ABSTRACT

In order to explore to what extent equilibrium adsorption can be studied with surface science methods such as reflection absorption infrared spectroscopy (RAIRS), static secondary ion mass spectroscopy (SSIMS) and X-ray photoelectron spectroscopy (XPS), adsorption of CO on a Rh(1 0 0) single crystal surface has been studied. A structural model of CO on Rh(1 0 0) at different coverages is presented. Under equilibrium adsorption conditions, we were able to determine the CO coverage and adsorption isotherms. From the isotherms, an isosteric heat of adsorption of about 160 kJ/mol was obtained, compared to an activation energy of desorption of 132 kJ/mol from temperature programmed desorption (TPD) experiments.

1. Introduction

In catalysis, one of the most important parameters predicting surface reactivity is the interaction energy between a molecule and the surface [1–3]. For validation of the accuracy of theoretical model, good quantitative data on adsorption energies is of significance. Several techniques are used in surface science studies to determine the adsorption energy. The most direct method is single crystal adsorption calorimetry (SCAC) [4,5], where the heat released during adsorption of a gas on an ultra-thin metal single crystal foil results in an increase of the foil temperature. A serious drawback is that the foils contain a high density of surface defects, which in turn affects the heat of adsorption. More widely employed is temperature programmed desorption (TPD). During TPD experiments, a metal single crystal with adsorbates is heated in a controlled fashion, often linearly with time, during which the desorption rate of the adsorbates is monitored with a mass spectrometer. Several methods have been derived from the Arrhenius equation to obtain an estimate of the kinetic parameters from the desorption traces, see [6,7] for a comparison between methods. A third technique is Clausius–Clapeyron analysis of equilibrium adsorption isosteres. In order to obtain the adsorption energy from equilibrium isosteres, the adsorbate coverage is measured in a gas atmosphere at different temperatures and pressures. In this case, it is not straightforward to determine the coverage, because the gas environment can affect the measurements.

In this paper, equilibrium isosteres are obtained with the surface science methods X-ray photoelectron spectroscopy (XPS), which is quantitative, and the semi-quantitative techniques: reflection absorption infra red spectroscopy (RAIRS) and static secondary ion mass spectroscopy (SSIMS). A comparison is made among the different techniques to determine how accurate coverages and adsorption energies are obtained with each technique. CO is used as a probe molecule to study the adsorption and desorption behaviour on a rhodium(1 0 0) single crystal surface. Although the adsorption of CO has been studied extensively [8–18], this is the first surface science study using as many as five different characterization techniques. First, CO is irreversible adsorbed at low temperatures and studied with low energy electron diffraction (LEED) and RAIRS. A structural model of CO on Rh(1 0 0) at different coverages is discussed, which is in excellent agreement with literature. The coverages belonging to the structural model are used to convert the areas under TPD traces into coverages, which in turn are correlated to the intensities observed in RAIRS, SSIMS and XPS experiments. Lastly, the adsorption/desorption equilibrium of CO is probed using XPS and the semi-quantitative techniques RAIRS and SSIMS to determine the adsorption energy by using the Clausius–Clapeyron equation. The resulting isosteric heat of adsorption is compared to the activation energy of desorption from TPD experiments.

We will now give a short review of previous results. LEED studies have shown that on Rh(1 0 0), CO orders into three distinct ordered structures at different coverages. Several studies [8–17] reported that CO orders in a $c(2 \times 2)$ structure at θ_{CO} = 0.50 ML. At

* Corresponding author. Tel.: +31 402474658; fax: +31 402473481.
E-mail address: M.M.M.Jansen@tue.nl (Maarten M.M. Jansen).

0920-5861/$ – see front matter © 2009 Elsevier B.V. All rights reserved.
doi:10.1016/j.cattod.2009.11.014

higher CO coverages, the $c(2 \times 2)$ converts into more compressed structures, leading to a $p(4\sqrt{2} \times \sqrt{2})R45^\circ$ structure at $\theta_{CO} = 0.75$ ML [8,10,11,13,15–17,19] and a $c(6 \times 2)$ structure [8,9,11,17] at the saturation coverage of 0.83 ML.

A combination of XPS [8,14,16] and two vibrational spectroscopy techniques electron energy loss spectroscopy (EELS) [10,15] and RAIRS [11,13,17] reveal how CO is bonded to the rhodium surface. Between $\theta_{CO} = 0$ and 0.50 ML, where CO orders into a $c(2 \times 2)$ structure, CO adsorbs mainly on top [8,10,11,15,16] with traces of bridge CO. Some studies report increased amounts of bridge bonded CO [13], which decreases when the temperature is raised [16]. This indicates the presence of (sub)surface contaminations [11]. From $\theta_{CO} = 0.5$ to 0.75 ML, the amount of bridge bonded CO increases caused by compression of the $c(2 \times 2)$ structure into the $p(4\sqrt{2} \times \sqrt{2})R45^\circ$ structure in which bridge bonded CO becomes more favourable. At $\theta_{CO} = 0.75$ ML, CO is present as a mixture of top and bridge bonded CO in a ratio of around 1:2, respectively [8,16]. At $\theta_{CO} = 0.83$ ML where CO is ordered in a $c(6 \times 2)$ pattern, RAIRS [11] shows only top bonded CO, whereas XPS [8,16] shows a mixture of CO on top and bridge sites.

Kinetic parameters for CO on Rh(1 0 0) have been determined with TPD [8,11,12,17,20], SCAC [21], reverse flash [22], single beam and modulated beam [23] experiments. TPD experiments show one desorption state at low coverage at around 500 K. At coverages above 0.50 ML, a low temperature shoulder grows in. From TPD spectra, activation energies of desorption ranging from 131 to 140 kJ/mol and preexponential factors from $10^{12.9}$ to $10^{14.1}$ were determined. With SCAC and the reverse flash method, a heat of adsorption of 118 and 121 kJ/mol, respectively was derived. Molecular beam studies resulted in values of 135 and 149 kJ/mol for single and modulated beams, respectively.

2. Experimental methods

Temperature programmed desorption, reflection absorption infra red spectroscopy [24–26], X-ray photoelectron spectroscopy [27,28] and low energy electron diffraction [29] experiments were carried out in a home built, two-stage stainless steel ultrahigh vacuum system with a base pressure of 1.5×10^{-10} mbar. The static secondary ion mass spectroscopy [30–32] experiments were carried out in a separate UHV system with a base pressure of 1×10^{-10} mbar (see Nieskens et al. [33] for further details).

In both set-ups TPD experiments were performed to determine the CO coverage (see de Jong and Niemantsverdriet [11] and refs therein). All TPD experiments were carried out with quadrupole mass spectrometers (Prisma QME200, Balzers) with a mass range (m/e) of 0–200 amu.

RAIRS spectra were taken with a Fourier-transform infrared spectrometer (Galaxy 4020, Mattson) flushed with dry nitrogen, such that the infrared beam undergoes a single reflection from the crystal surface near grazing angle (85°). A wire grid polarizer is placed in the beam allowing only the p-polarized component of the light to be detected. RAIRS observes only vibrations of atoms and molecules with a vertical component by absorption of p-polarized light. A mercury cadmium telluride (MCT) detector was used with a spectral range of 4000–800 cm^{-1}. All spectra consist of 512 scans taken at 4 cm^{-1} spectral resolution divided by a stored background spectrum of a clean surface at 300 K.

XPS experiments were performed with a VG100AX spectrometer (VG Microtech) consisting of a twin anode (Al/Mg) X-ray source at an incident polar angle of 60° with respect to the surface normal and the 100 mm hemispherical analyzer perpendicular to the surface. In three regions 540–510 eV O 1s, 325–300 eV Rh 3d and 300–275 eV C 1s spectra were obtained with a pass energy of 50 eV for Rh 3d and 100 eV O 1s and C 1s. The O 1s, Rh 3d, and C 1s spectra were recorded in 15, 2, and 12.5 min, respectively.

SIMS measurements were performed using a Balzers QMA400 mass spectrometer and a differentially pumped ion gun (SPECS PU-IQE 12/38). Static SIMS spectra were obtained by using a defocused 5 keV argon primary ion beam with a current density of 1 nA/cm^{-2} at an incident polar angle of 65°. Secondary ions were collected under a polar angle of 25°. These conditions enable measurements in static mode, with a removal rate of one monolayer per hour. A typical experiment lasts less than 5 min.

LEED experiments have been carried out using a reverse-view two grid mini-LEED system (BDL450IR, OCI Vacuum Microengineering) with external retraction. The electron beam had a beam current of 0.50 μA and beam energy between 85 and 95 eV. LEED patterns are acquired and digitized using a CCD camera (Cohu), connected to a computer for analysis and storage of images.

Two similar rhodium single crystals of (1 0 0) orientation with a thickness of 1.2 mm were mounted in each system on a movable sample rod by two tantalum wires of 0.3 mm diameter, pressed into small grooves on the side of the crystal. This set-up allowed for resistive heating up to 1400 K. The sample was continuously cooled with liquid nitrogen enabling temperatures as low as 88 K. Temperatures were measured using a chromel–alumel thermocouple spot-welded to the back of the crystal.

The crystal surface was cleaned by cycles of argon ion sputtering and annealing in an oxygen atmosphere. Argon ion sputtering (6 μA/cm^2) at 920 K was used to remove impurities, such as boron, sulphur, phosphorus, and chlorine. Near-surface carbon was removed in 2×10^{-8} mbar O_2 at temperatures ranging from 900 to 1100 K. Oxygen was removed by flashing to 1400 K. After flashing, a small amount of O_2 was adsorbed and flashed to 800 K to remove carbon diffusing to the surface at temperatures above 900 K. Finally CO was dosed at 550 K and flashed to 800 K to remove excess oxygen. Carbon monoxide (Hoek Loos, 99.997% pure) was used without further purification.

3. Results and discussion

First, the behaviour of CO on Rh(1 0 0) at low temperatures is discussed. Results from LEED and RAIRS experiments are presented. Second, the coverages obtained from TPD experiments are related to intensities observed in RAIRS, SSIMS, and XPS experiments. Lastly, RAIRS, SSIMS, and XPS results on the adsorption/desorption equilibrium of CO on Rh(1 0 0) are presented.

3.1. CO on Rh(1 0 0) at low temperatures

Fig. 1 shows an overview of the LEED patterns that arise at various CO coverages. CO was adsorbed at 150 K by exposing the crystal surface to 1×10^{-8} mbar CO. Models for the CO overlayer structures are adopted from de Jong and Niemantsverdriet [11] and from Eichler and Hafner [34]. A $p(1 \times 1)$ LEED pattern of the bare Rh(1 0 0) surface is shown on the left. The first LEED pattern originating from ordered CO is observed between 0.30 and 0.50 ML CO: a clear $c(2 \times 2)$ pattern is formed [8–16]. A $p(4\sqrt{2} \times \sqrt{2})R45^\circ$ structure is shown in the third panel. This structure occurs when the $c(2 \times 2)$ overlayer is compressed and it is most explicit at a coverage of 0.75 ML at 300 K. An increased CO pressure of 1×10^{-7} mbar at 150 K was used to further compress the CO layer forming a $c(6 \times 2)$ structure at $\theta_{CO} = 0.83$ ML as shown on the right. For calibrating SSIMS, RAIRS and XPS a saturation coverage of 0.75 ML is used as a reference: a CO pressure of 1×10^{-8} mbar is used at which the $p(4\sqrt{2} \times \sqrt{2})R45^\circ$ structure is observed.

Fig. 2 shows the RAIRS spectra of CO on Rh(1 0 0) at different coverages. Each spectrum was obtained after exposing the

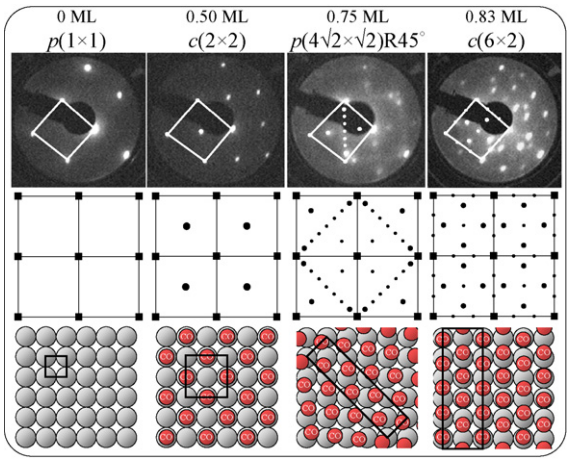

Fig. 1. Low energy electron diffraction patterns of several coverages of CO adsorbed on Rh(1 0 0) at 150 K. The beam energy used is between 85 and 93 eV.

crystal to CO at 150 K and subsequently heating to 300 K to dispose of co-adsorbed hydrogen. Hereafter, a TPD experiment was performed to obtain the coverage. The RAIRS spectra show two absorption bands in the regions 1870–1944 cm^{-1} and 1997–2055 cm^{-1}, in good agreement with reported EELS [10,15] and previous RAIRS [11,17] studies. These bands were assigned to top and bridge bonded CO, respectively. At coverages up to 0.5 ML, absorption by CO on top sites increases and the absorption band shifts to higher frequencies. Absorption by bridge bonded CO is very weak. CO orders into a $c(2 \times 2)$ structure mainly occupying top sites as shown in Fig. 1.

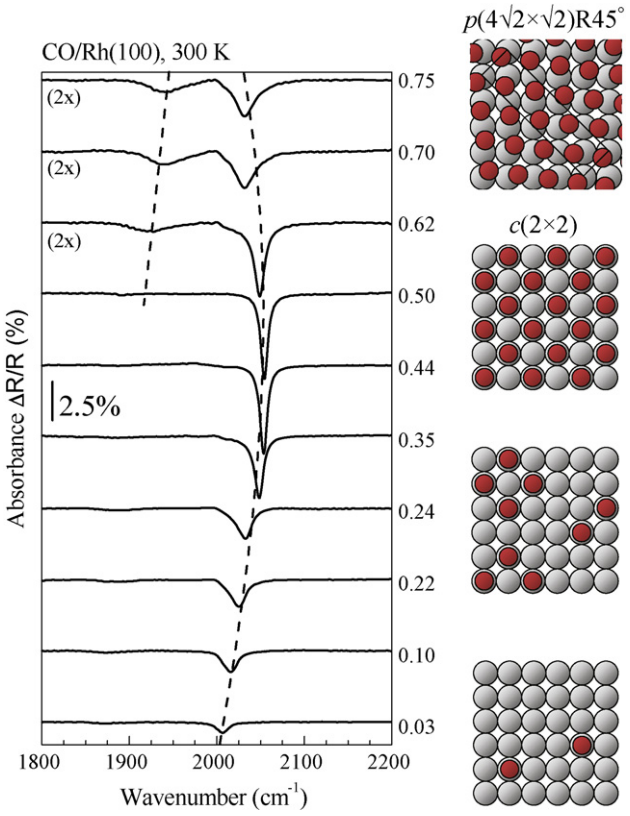

Fig. 2. Reflection absorption infra red spectra obtained after exposing the Rh(1 0 0) surface to various doses of CO at 150 K with subsequently heating to 300 K.

The frequency shift can be attributed to lateral interactions between the CO molecules, resulting in both vibrational coupling and static effects [24,25]. Vibrational coupling within an adsorbate layer takes place through direct dipole–dipole coupling (i.e. through space) and via coupling of metal electrons. Increasing the coverage increases resonance between the vibrating dipoles, which in turn increases the frequency and amplifies the absorption intensity. Static effects or chemical shifts can be understood with the back-bonding model of Blyholder [35]: while electrons are donated into the anti-bonding orbitals of the CO molecule the CO stretching frequency decreases. A high coverage may cause the CO molecules to compete for the metal electrons, resulting in lower back-donation, and hence, the CO stretching frequency shifts toward higher frequencies. Persson and Ryberg [36] reported that the increase in stretching frequency of CO on transition metals is predominantly caused by dipole–dipole coupling.

Above θ_{CO} = 0.5 ML, the intensity of the linear band decreases while concurrently an increase in intensity of the bridge band is observed. This can be attributed to the transition from a $c(2 \times 2)$ into a more condensed $p(4\sqrt{2} \times \sqrt{2})R45^\circ$ overlayer structure[10]. The amount of linear bonded CO decreases from 0.5 ML in the case of a completely ordered $c(2 \times 2)$ structure to 0.25 ML in a completely ordered $p(4\sqrt{2} \times \sqrt{2})R45^\circ$ layer, while the amount of bridge bonded CO increases from ~0 ML to 0.5 ML.

Fig. 3 shows the relation between the CO coverage and the CO stretching frequency. Up to θ_{CO} = 0.5 ML, the frequency of both CO on top and bridge sites increases with increasing coverage, mainly caused by an increase in dipole–dipole interactions between CO molecules. Above θ_{CO} = 0.5 ML, the stretching frequency of bridge bonded CO increases while concurrently the frequency of top CO decreases. During formation of the $p(4\sqrt{2} \times \sqrt{2})R45^\circ$ overlayer structure, the amount of top CO decreases and becomes diluted in an adlayer with mainly bridge bonded CO. This results in a decrease in dipole–dipole coupling between the CO molecules on top sites.

The decrease in frequency of CO on top sites from 2050 cm^{-1} at 0.50 ML to 2030 cm^{-1} at 0.75 ML is not found in earlier RAIRS studies [11,13]. At θ_{CO} = 0.75 ML, de Jong and Niemantsverdriet report two bands at 2070 and 2030 cm^{-1} on top sites. An adsorption temperature of 300 K was used in this study, while we adsorbed CO at 150 K. The difference in adsorption temperature has an influence on the coverage and on the degree of ordering. Two CO structures may be present in the study reported by de Jong and Niemantsverdriet with patches of the $p(4\sqrt{2} \times \sqrt{2})R45^\circ$ and $c(2 \times 2)$ structure causing adsorption bands at 2030 cm^{-1} and 2070 cm^{-1}, respectively.

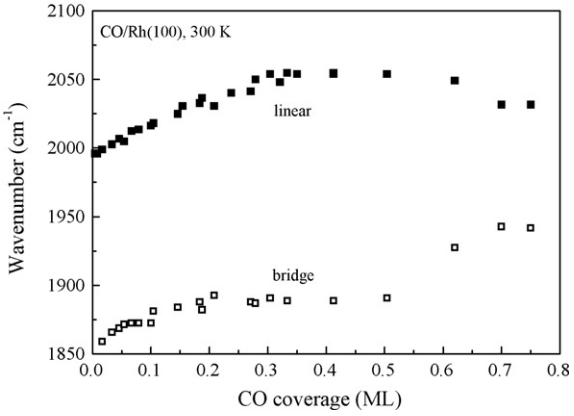

Fig. 3. The CO stretching frequency as a function of the CO coverage on Rh(1 0 0) at 300 K.

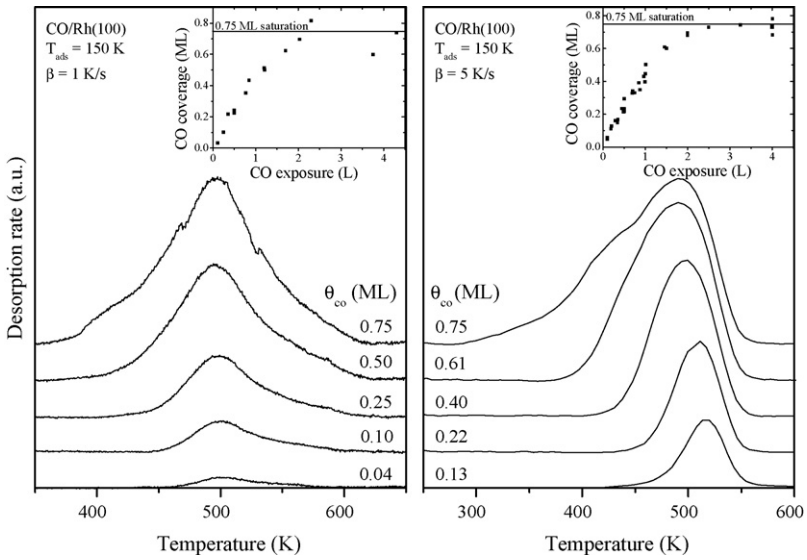

Fig. 4. Temperature programmed desorption spectra of CO adsorbed on Rh(1 0 0) at 150 K at several coverages. The heating rates are 1 K/s (left) and 5 K/s (right). Uptake curves are shown as insets.

3.2. Linking RAIRS, SSIMS and XPS intensities to the CO coverage

First, TPD results of CO on Rh(1 0 0) are presented to obtain a direct relation between the CO exposure and CO coverage. The CO coverage is proportional to the area under the desorption traces and the CO saturation coverage of 0.75 ML was used as a reference to scale all CO coverages. Secondly, we will establish a link between the CO coverage and the intensities obtained by RAIRS, SSIMS and XPS experiments. The relevant RAIRS intensity that shows a strong correlation with the CO coverage is the integrated absorption intensity of CO molecules on top sites; the relevant intensity for SSIMS is the intensity ratio between $(RhCO)^+$ and $(Rh)^+$ ions; and the relevant XPS intensity is the photoelectron intensity ratio between the oxygen 1s and rhodium $3d_{5/2}$ peak.

Fig. 4 shows the CO desorption spectra on Rh(1 0 0) at different CO coverages from the RAIRS set-up (left) and the SSIMS set-up (right). The crystal was exposed to 1×10^{-8} mbar CO at 150 K. Up to 0.5 ML, a single CO desorption state is observed around 500 K which shifts to a lower temperature at increasing coverage. CO is present as a stable top species with $c(2 \times 2)$ ordering between 0.3 and 0.5 ML, see Fig. 2. Above 0.5 ML, a low temperature shoulder is being formed, indicating destabilization of CO in the compressed $p(4\sqrt{2} \times \sqrt{2})R45^\circ$ overlayer structure.

By applying the Chan–Aris–Weinberg (CAW1/2) method for first order desorption kinetics [37], an activation energy and preexponential factor for CO desorption of 132 kJ/mol and $10^{12.7}$ s^{-1} in the zero-coverage limit is obtained. These values agree well with other TPD studies: Kim et al. [12] acquired an activation energy of 133 kJ/mol and a preexponential factor of $10^{12.9}$ s^{-1} and de Jong and Niemantsverdriet [11] found values of E_{ads} = 131 kJ/mol and $\nu = 10^{13.9}$ s^{-1}, respectively.

The insets of Fig. 4 show the CO uptake curves: the relation between the exposure of the crystal surface to CO and the resulting CO coverage. This relation is used to relate the RAIRS, SSIMS, and XPS intensities to the coverage.

Fig. 5(left) shows the infrared absorption intensity of Fig. 2 as a function of the CO coverage. The integrated absorption intensities of CO on top and bridge sites are plotted. Initially, absorption by CO on top sites increases strongly. An increase in the CO coverage and formation of the $c(2 \times 2)$ structure results in more interacting

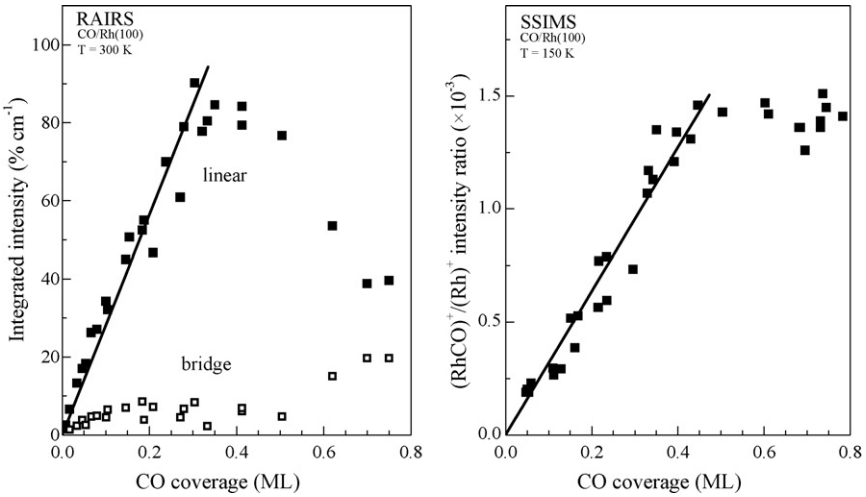

Fig. 5. (Left) Integrated absorption intensities of the CO bands as a function of CO coverage obtained with RAIRS. (Right) Static secondary ion mass spectrometry intensity ratios as a function of CO coverage. CO was adsorbed at 150 K.

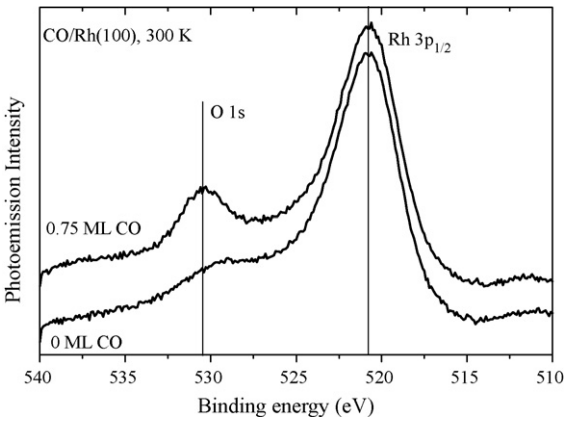

Fig. 6. X-ray photoemission spectra of 0 and 0.75 ML CO on the Rh(1 0 0) surface. CO was adsorbed at 150 K and the surface was subsequently heated to 300 K.

neighbouring CO molecules at $\sqrt{2}$ times the Rh-Rh distance, which in turn increases dipole–dipole coupling. Between θ_{CO} = 0.3 and 0.5 ML, the absorption intensity stays constant and a sharpening of the band is observed in Fig. 2. Above θ_{CO} = 0.5 ML, the absorption by CO on top sites decreases, whereas an increase in absorption by bridge bonded CO is observed. This is due to the partial migration of CO on top sites in the $c(2 \times 2)$ overlayer structure onto bridge positions in the $p(4\sqrt{2} \times \sqrt{2})R45^\circ$ structure.

In the region between 0 and 0.3 ML, absorption by CO on top sites increases mainly linearly. Hence, the absorption intensity obtained with RAIRS of top CO is a good measure of the CO coverage. This relation is used in Fig. 7a.

Fig. 5(right) shows the correlation between the SSIMS intensity and coverage. Each experiment was done by first exposing the crystal to CO, second monitoring the ion intensities of $(Rh)^+$ (m/e = 103) and $(RhCO)^+$ (m/e = 131) for 20 s, after which a TPD experiment followed. To exclude influences from changes in the sample position, $(RhCO)^+/(Rh)^+$ ion intensity ratios are used.

Between 0 and 0.4 ML, a linear increase in the ion intensity ratio is observed, while above 0.45 ML it stays constant. The $(Rh)^+$ region is very sensitive to the concentration of top bonded species as the $(Rh_2)^+$ region is more sensitive for higher coordinated adsorbed species [38–40] like bridge and hollow CO. The change in ordering from the $c(2 \times 2)$ into $p(4\sqrt{2} \times \sqrt{2})R45^\circ$ overlayer structure is accompanied by a decrease in CO on top sites towards bridge CO. This could cause the intensity ratio to be constant in our case above θ_{CO} = 0.45 ML.

The ion intensity ratio is generally a semi-quantitative indicator of the coverage [31,41–44]. The mass intensity ratio increases linearly with CO coverage up to 0.45 ML. Hence, between θ_{CO} = 0 and 0.45 ML, the $(RhCO)^+/(Rh)^+$ ion intensity ratio is a good measure of the CO coverage.

XPS is known for determination of surface compositions quantitatively. A well documented linear relationship exists between the XPS intensity and the concentration of an element [27,28,45]. In our case we use the surface oxygen concentration to determine the CO coverage. To avoid influences of changes in sample position, the integrated intensity ratio of the oxygen 1s state to the rhodium $3d_{5/2}$ state is used. The intensities of two well defined coverages are used in this paper: θ_{CO} = 0 and 0.75 ML to construct a linear plot of the CO coverage and the intensity. Fig. 6 shows the XPS spectra of a clean Rh(1 0 0) surface (θ_{CO} = 0 ML) and a surface covered with 0.75 ML CO. The spectra were obtained at 300 K after exposing the crystal to CO at 150 K. Even on clean Rh(1 0 0), a small feature in the oxygen 1s region is present due to shake-up satellite peaks. To determine the integrated intensity of the rhodium $3d_{5/2}$ state and the oxygen 1s state, a Shirley or linear background was used after which each state was fitted by one peak with 70% Gaussian and 30% Lorentzian characteristics.

3.3. Equilibrium CO adsorption/desorption on Rh(1 0 0)

The equilibrium between adsorption and desorption of CO was studied with RAIRS, SSIMS, and XPS. Fig. 7 shows sets of isotherms, where the CO coverage on Rh(1 0 0) is described as a function of the

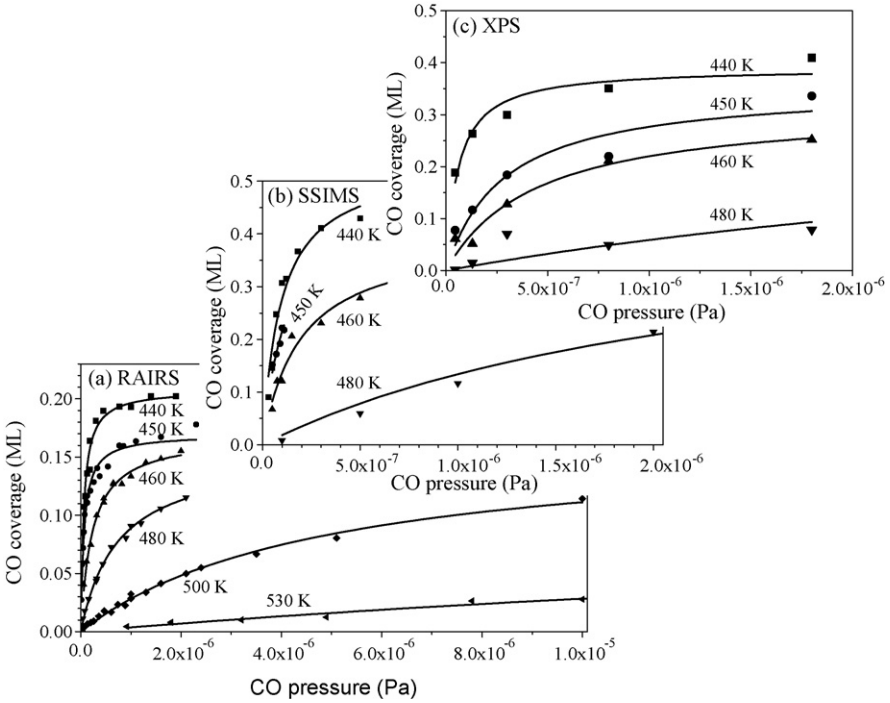

Fig. 7. Adsorption isotherms of CO on Rh(1 0 0) at different temperatures measured with: (a) RAIRS; (b) SSIMS; and (c) XPS. The CO coverage was determined after 25 min of exposure of CO at a constant pressure and temperature.

CO pressure at a constant temperature. After 25 min of exposure to CO, equilibrium between gas phase and adsorbed CO was reached after which the coverage was determined. In general, the isotherm initially increases linearly with pressure and levels off near saturation. At higher temperatures, lower coverages are observed due to the shift in equilibrium towards higher desorption rates. In all three cases, the adsorption isotherms deviate from Langmuir type of adsorption behaviour, because Langmuir adsorption isotherms assume equivalent adsorption sites and no lateral interactions. For CO on Rh(1 0 0), this is only valid at very low coverages where CO is randomly distributed. Deviations from Langmuir behaviour occur mainly due to lateral interactions and difference in stability of adsorption sites. For example, the interaction energy between two neighbouring CO molecules on top sites was determined with Monte-Carlo simulations to be 9 kJ/mol by Kose et al. [21] and 24 kJ/mol by Jansen [46]. In addition, CO occupying a bridge site is 4.6 kJ/mol less stable than CO on the top site [10].

The CO adsorption isotherms obtained with XPS and SSIMS display similar behaviour, although coverages determined with SSIMS are slightly higher. The small differences in CO coverage are probably caused by the insensitivity of the XPS apparatus resulting in lower accuracy in determining the CO coverage, especially at lower coverages. The use of two UHV apparatus with different types of pressure meters also contributes to differences in measured pressure and the actual pressure near the crystal surface.

The CO adsorption isotherms were also determined with RAIRS. In all experiments, an intense absorption band by CO on top sites was observed while the band for bridge bonded CO was very weak, indicating that only using absorption of top CO is a valid assumption to obtain the CO coverage. The isotherms at 440 and 450 K show initially a very steep linear increase in the coverage with the pressure, but there is an abrupt levelling of the CO coverage at higher pressures. The initial linear parts of the isotherms are comparable with SSIMS and XPS results, while the part of the isotherms at higher pressures deviate and lower coverages are obtained. The linear relation between the coverage and the integrated RAIRS intensity as shown in Fig. 5 is perhaps not completely applicable at all temperatures, but a correlation as in Fig. 8 is more accurate. The saturation of the integrated intensity at higher temperatures is probably caused by the increase in CO diffusion rates at higher temperatures. Higher diffusion rates lead to more collisions between molecules on the surface, resulting in more repulsive lateral interactions between CO molecules at a similar coverage. This leads to a weaker Rh–C bond, reducing backdonation into the anti-bonding orbitals of the CO molecule, which depolarizes the CO molecule. This effect has also been reported by Hoffmann [25].

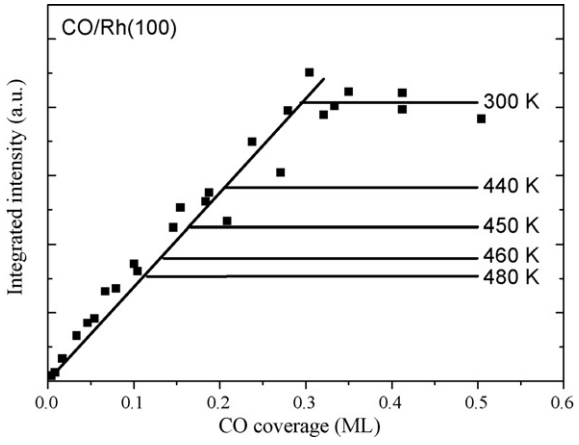

Fig. 8. Integrated absorption intensities of the linear CO band as a function of coverage for CO adsorbed on Rh(1 0 0) at different temperatures.

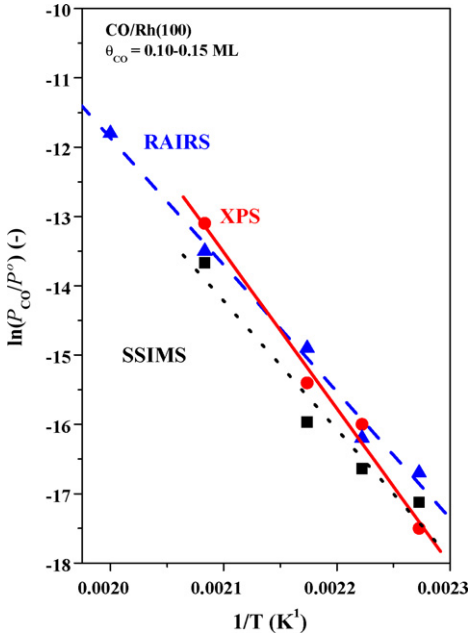

Fig. 9. Adsorption isosteres of CO on Rh(1 0 0). The slope equals the enthalpy of adsorption divided by *R*. The results obtained with RAIRS, SSIMS and XPS are plotted.

Fig. 7 shows the adsorption isotherms as a function of temperature. From these equilibrium experiments the isosteric heat of adsorption can be obtained. The adsorption energy is closely approximated by the enthalpy of adsorption and can be obtained with the Clausius–Clapeyron equation:

$$\left(\frac{\partial \ln(p_{CO}/p^{o})}{\partial(1/T)}\right)_{\theta_{CO}=\text{constant}} \approx -\frac{\Delta H_{ads}}{R} \quad (1)$$

To apply the Clausius–Clapeyron equation, a plot of $\ln(p_{CO}/p^{o})$ versus $1/T$ is made at a constant CO coverage. A linear relation is observed with the slope as the enthalpy of adsorption divided by the gas constant *R*. Fig. 9 shows the resulting adsorption isosteres.

With SSIMS, an adsorption isostere was obtained at 0.15 ML, while 0.10 ML was used with RAIRS and XPS. SSIMS and RAIRS give similar plots: they are equal in slope corresponding to an adsorption energy of about 152–155 kJ/mol, but the isostere from SSIMS is lying slightly lower. The isostere obtained with XPS has a slightly larger slope, resulting in a higher adsorption energy of 175 kJ/mol, as reflected in Table 1. This can be caused by the insensitivity of our XPS detector or by the decrease in sensitivity of the electron multiplier at higher CO pressures.

Table 1
The adsorption energies of CO on Rh(1 0 0) determined by using the Clausius–Clapeyron equation. Adsorption isosteres were determined with RAIRS, SSIMS and XPS. Results from other techniques are included as a reference.

Technique	ΔE_{ads} (kJ/mol)
RAIRS	152 ± 9
SSIMS	155 ± 5
XPS	175 ± 10
TPD [8,11,12,20]	131–140
Single beam [23]	135 ± 8
Modulated beam [23]	149 ± 10
SCAC [21]	118
Reverse flash [22]	121

Table 1 shows the adsorption enthalpies obtained under equilibrium conditions and from various other techniques. By using equilibrium conditions, relatively high adsorption energies are obtained. So far, DFT simulations fail to predict the adsorption energy of CO on various transition metals correctly – including rhodium – due to overestimating the interaction of the LUMO with the metal substrate [47]. Recently, more sophisticated approaches have been developed which correct for overbinding more efficiently. With this approach, the adsorption energy of CO on Rh(1 0 0) on the for DFT most stable bridge site was reported to be 175 kJ/mol by Hammer et al. [48] and 178 kJ/mol by Van Bavel et al. [20].

4. Conclusions

We have explored to what extent equilibrium adsorption isosteres can be measured using common surface science methods such as RAIRS, SSIMS and XPS. We have investigated adsorption and desorption behaviour of CO on the surface of a Rh(1 0 0) single crystal. Below 300 K, CO adsorbs mainly linear up to θ_{CO} = 0.50 ML ordering into a $c(2 \times 2)$ structure. Between θ_{CO} = 0.50 and 0.75 ML, the amount of CO on top sites decreases, whereas the amount of bridge bonded CO increases forming a $p(4\sqrt{2} \times \sqrt{2})R45^{\circ}$ structure at θ_{CO} = 0.75 ML. CO desorbs between 350 and 550 K, with one main desorption peak around 500 K for the $c(2 \times 2)$ structure and a low temperature shoulder around 450 K for the $p(4\sqrt{2} \times \sqrt{2})R45^{\circ}$ structure. An adsorption energy of 132 kJ/mol was determined with TPD experiments.

With RAIRS, SSIMS, and XPS the adsorption/desorption equilibrium of CO was studied obtaining adsorption isotherms between 440 and 530 K. Similar coverages were obtained with SSIMS and XPS, whereas unexpected deviations are found for the isotherms resulting from RAIRS. Absorption of infrared light by linear bonded CO used to determine the CO coverage with RAIRS correlate differently with coverage at 300 K compared to temperatures of 440–530 K. This makes RAIRS only employable to determine the CO coverage accurately in a limited coverage range. The adsorption energy obtained from equilibrium isosteres was about 160 kJ/mol and is relatively high compared to 132 kJ/mol obtained with TPD.

In general, we show that equilibrium adsorption isotherms can be measured in the low coverage domain when lateral interactions are absent, and when spectroscopic observables vary linearly with coverage.

References

[1] F. Studt, F. Abild-Pedersen, T. Bligaard, R.Z. Sorensen, C.H. Christensen, J.K. Nørskov, Identification of non-precious metal alloy catalysts for selective hydrogenation of acetylene, Science 320 (2008) 1320–1322.
[2] J.K. Nørskov, et al., Universality in heterogeneous catalysis, J. Catal. 209 (2002) 275–278.
[3] Z.P. Liu, P. Hu, General trends in the barriers of catalytic reactions on transition metal surfaces, J. Chem. Phys. 115 (2001) 4977–4980.
[4] W.A. Brown, R. Kose, D.A. King, Femtomole adsorption calorimetry on single-crystal surfaces, Chem. Rev. 98 (1998) 797–831.
[5] S. Cerny, Adsorption microcalorimetry in surface science studies sixty years of its development into a modern powerful method, Surf. Sci. Rep. 26 (1996) 1–59.
[6] J.B. Miller, H.R. Siddiqui, S.M. Gates, J.N. Russell, J.T. Yates, J.C. Tully, M.J. Cardillo, Extraction of kinetic parameters in temperature programmed desorption: a comparison of methods, J. Chem. Phys. 87 (1987) 6725–6732.
[7] D.L.S. Nieskens, A.P. van Bavel, J.W. Niemantsverdriet, The analysis of temperature programmed desorption experiments of systems with lateral interactions; implications of the compensation effect, Surf. Sci. 546 (2003) 159–169.
[8] A. Baraldi, L. Gregoratti, G. Comelli, V.R. Dhanak, M. Kiskinova, R. Rosei, CO adsorption and CO oxidation on Rh(1 0 0), Appl. Surf. Sci. 99 (1996) 1–8.
[9] D.G. Castner, B.A. Sexton, G.A. Somorjai, LEED and thermal desorption studies of small molecules (hydrogen, oxygen, carbon monoxide, carbon dioxide, nitric oxide, ethene, ethyne and carbon) chemisorbed on the rhodium (1 1 1) and (1 0 0) surfaces, Surf. Sci. 71 (1978) 519–540.
[10] B.A. Gurney, L.J. Richter, J.S. Villarrubia, W. Ho, The populations of bridge and top site carbon monoxide on rhodium(1 0 0) vs. coverage, temperature, and during reaction with atomic oxygen, J. Chem. Phys. 87 (1987) 6710–6721.
[11] A.M. de Jong, J.W. Niemantsverdriet, The adsorption of CO on Rh(1 0 0): reflection absorption infrared spectroscopy, low energy electron diffraction, and thermal desorption spectroscopy, J. Chem. Phys. 101 (1994) 10126–10133.
[12] Y. Kim, H.C. Peebles, J.M. White, Adsorption of deuterium, carbon monoxide and the interaction of co-adsorbed deuterium and carbon monoxide on rhodium (1 0 0), Surf. Sci. 114 (1982) 363–380.
[13] L.W.H. Leung, J.W. He, D.W. Goodman, Adsorption of CO on Rh(1 0 0) studied by infrared reflection-absorption spectroscopy, J. Chem. Phys. 93 (1990) 8328–8336.
[14] T. Ramsvik, A. Borg, M. Kildemo, S. Raaen, A. Matsuura, A.J. Jaworowski, T. Worren, M. Leandersson, Molecular vibrations in core-ionised CO adsorbed on Co(0 0 0 1) and Rh(1 0 0), Surf. Sci. 492 (2001) 152–160.
[15] L.J. Richter, B.A. Gurney, W. Ho, The influence of adsorbate–adsorbate interactions on surface structure: the coadsorption of carbon monoxide and molecular hydrogen on rhodium(1 0 0), J. Chem. Phys. 86 (1987) 477–490.
[16] F. Strisland, A. Ramsted, T. Ramsvik, A. Borg, CO adsorption on the Rh(1 0 0) surface studied by high resolution photoelectron spectroscopy, Surf. Sci. 415 (1998) L1020–L1026.
[17] M.M.M. Jansen, B.E. Nieuwenhuys, D. Curulla-Ferre, J.W. Niemantsverdriet, Influence of nitrogen atoms on the adsorption of CO on a Rh(1 0 0) single crystal surface, J. Phys. Chem. C 113 (2009) 12277–12285.
[18] D.L.S. Nieskens, M.M.M. Jansen, A.P. van Bavel, D. Curulla-Ferre, J.W. Niemantsverdriet, The influence of carbon on the adsorption of CO on a Rh(1 0 0) single crystal, Phys. Chem. Chem. Phys. 8 (2006) 624–632.
[19] C.W. Tucker, Chemisorbed coincidence lattices on rhodium, J. Appl. Phys 37 (1966) 3013–3019.
[20] A.P. van Bavel, M.J.P. Hopstaken, D. Curulla, J.W. Niemantsverdriet, J.J. Lukkien, P.A.J. Hilbers, Quantification of lateral repulsion between coadsorbed CO and N on Rh(1 0 0) using temperature-programmed desorption, low-energy electron diffraction, and Monte Carlo simulations, J. Chem. Phys. 119 (2003) 524–532.
[21] R. Kose, W.A. Brown, D.A. King, Role of lateral interactions in adsorption kinetics: CO/Rh{1 0 0}, J. Phys. Chem. B 103 (1999) 8722–8725.
[22] V.K. Medvedev, V.S. Kulik, V.I. Chernyi, Y. Suchorski, Weakly chemisorbed CO layer on Rh (1 0 0) as detected by reverse flash and field ion appearance energy measurements, Vacuum 48 (1997) 341–345.
[23] D.H. Wei, D.C. Skelton, S.D. Kevan, Desorption and molecular interactions on surfaces: CO/Rh(110), CO/Rh(1 0 0) and CO/Rh(111), Surf. Sci. 381 (1997) 49–64.
[24] Y.J. Chabal, Surface infrared spectroscopy, Surf. Sci. Rep 8 (1988) 211–357.
[25] F.M. Hoffmann, Infrared reflection-absorption spectroscopy of adsorbed molecules, Surf. Sci. Rep. 3 (1983) 107–192.
[26] P. Hollins, J. Pritchard, Infrared Studies of chemisorbed layers on single crystals, Prog. Surf. Sci. 19 (1985) 275–350.
[27] D. Briggs, M.P. Seah, Practical Surface Analysis: Auger and X-ray Photoelectron Spetroscopy, Wiley, New York, 1996.
[28] S. Hüfner, Photoelectron Spectroscopy – Principles and Applications, Springer, Berlin, 1996.
[29] G. Ertl, J. Küppers, Low Energy Electrons and Surface Chemistry, VCH, Weinheim, 1985.
[30] A. Benninghoven, F.G. Rüdenauer, H.W. Werner, Secondary Ion Mass Spectrometry, Basic Concepts, Instrumental Aspects, Applications and Trends, Wiley, New York, 1987.
[31] D. Briggs, A. Brown, J.C. Vickerman, Handbook of Static Secondary Ion Mass Spectrometry, Wiley, Chichester, 1989.
[32] J.C. Vickerman, A. Brown, N.M. Reed, Secondary Ion Mass Spectrometry: Principles and Applications, Clarendon, Oxford, 1989.
[33] D.L.S. Nieskens, A.P. van Bavel, D. Curulla-Ferre, J.W. Niemantsverdriet, Ethylene decomposition on Rh(1 0 0): theory and experiment, J. Phys. Chem. B 108 (2004) 14541–14548.
[34] A. Eichler, J. Hafner, Adsorption of CO on Rh(1 0 0) studied by ab initio local-density functional calculations, J. Chem. Phys. 109 (1998) 5585–5595.
[35] G. Blyholder, Molecular orbital view of chemisorbed carbon monoxide, J. Phys. Chem. 68 (2002) 2772–2777.
[36] B.N.J. Persson, R. Ryberg, Vibrational interaction between molecules adsorbed on a metal surface: the dipole–dipole interaction, Phys. Rev. B: Condens. Matter 24 (1981) 6954–6970.
[37] C.M. Chan, R. Aris, W.H. Weinberg, An analysis of thermal desorption mass spectra. I, Appl. Surf. Sci. 1 (1978) 360–376.
[38] A. Brown, J.C. Vickerman, Surface coverage measurements for carbon monoxide adsorption on ruthenium(0 0 1): a combined SIMS/TPD study, Vacuum 31 (1981) 429–433.
[39] A. Brown, J.C. Vickerman, SIMS studies of adsorbate structure. I. Carbon monoxide adsorption on ruthenium(0 0 1), nickel(1 1 1), and nickel(1 0 0), Surf. Sci. 117 (1982) 154–164.
[40] A. Brown, J.C. Vickerman, Static SIMS studies of adsorbate structure. II. Carbon monoxide adsorption on palladium(1 1 1); adsorbate-adsorbate interactions on ruthenium(0 0 1), nickel(1 1 1) and palladium(1 1 1), Surf. Sci. 124 (1983) 267–278.
[41] A. Benninghoven, P. Beckmann, D. Greifendorf, K.H. Mueller, M. Schemmer, Hydrogen detection by secondary ion mass spectroscopy: hydrogen on polycrystalline nickel, Surf. Sci. 107 (1981) 148–164.
[42] H.J. Borg, J.W. Niemantsverdriet, Applications of secondary ion mass spectrometry in catalysis and surface chemistry, Catalysis: A Specialist Periodical Report 11 (1994) 1–50.
[43] L.L. Lauderback, W.N. Deglass, Secondary ion mass spectrometry of the ethylene/ruthenium(0 0 1) interaction, ACS Symp. Ser. 248 (1984) 21–37.

[44] X.Y. Zhu, J.M. White, Hydrogen interaction with nickel(1 0 0): a static secondary ion mass spectroscopy study, J. Phys. Chem. B 92 (1988) 3970–3974.
[45] G.C. Smith, Surface Analysis by Electron Spectroscopy: Measurement and Interpretation, Plenum, New York, 1994.
[46] A.P.J. Jansen, Monte Carlo simulations of temperature-programmed desorption spectra, Phys. Rev. B 69 (2004), 035414/1–035414/6.
[47] G. Kresse, A. Gil, P. Sautet, Significance of single-electron energies for the description of CO on Pt(1 1 1), Phys. Rev. B: Condens. Matter Mater. Phys. 68 (2003), 073401/1–073401/4.
[48] B. Hammer, L.B. Hansen, J.K. Norskov, Improved adsorption energetics within density-functional theory using revised Perdew–Burke–Ernzerhof functionals, Phys. Rev. B: Condens. Matter Mater. Phys. 59 (1999) 7413–7421.